

Design and Self-Assembly of Cavity-Containing Rectangular Grids

Leonard R. MacGillivray, Ryan H. Groeneman, and
Jerry L. Atwood*

Department of Chemistry
University of Missouri—Columbia
Columbia, Missouri 65211

Received October 15, 1997
Revised Manuscript Received January 29, 1998

It is becoming increasingly clear that transition-metal-based self-assembly processes that utilize *exo*-bidentate bridging ligands for propagating the coordination geometries of metals¹ can lead to functional supramolecular frameworks that exhibit interesting inclusion phenomena, molecular recognition properties, and unique forms of isomerism.^{1,2} In this context, discrete (e.g., molecular squares)³ and infinite (e.g., 2D grids)⁴ square assemblies have attracted much interest owing to their ability to form cavities capable of entrapping electron-rich guests (e.g., aromatics) with high shape selectivity.^{3c,4a} Despite the syntheses of these square frameworks, however, the design of related rectangular assemblies has, to our knowledge, remained elusive.⁵

Here, we now present a design strategy for the construction of cavity-containing rectangular frameworks and the one-pot synthesis of the first cavity-containing metal–organic rectangular grids, $[M(4,4'\text{-bipy})(\text{pyca})(\text{H}_2\text{O})_2]^+ \mathbf{1}$ (where M = Co(II) **1a**, Cd(II) **1b**; 4,4'-bipy = 4,4'-bipyridine; pyca = pyridine-4-carboxylate; Hpyca = pyridine-4-carboxylic acid). We demonstrate the ability of **1** to self-assemble in the solid state to form stacked layers in which hydrogen bonds and π – π interactions between the grids induce their alignment. As a consequence of these interactions, interconnected microchannels, which run approximately perpendicular to the grids, have formed and are observed to accommodate charged and neutral guests.

Our strategy for the construction of cavity-containing rectangular assemblies lies with the recognition that their frameworks must be designed such that they possess two unique edge lengths. This means that two unique spacer units must be incorporated within the framework which, in principle, can be achieved using neutral and/or charged bridging ligands. Indeed, a route that exploits the principles of self-assembly is desirable, since the framework can be attained in a single step and, typically, in high yield.^{2a}

(1) Hennigar, T. L.; MacQuarrie, D. C.; Losier, P.; Rogers, R. D.; Zaworotko, M. J. *Angew. Chem., Int. Ed. Engl.* **1997**, *36*, 972.

(2) (a) Stang, P. J.; Persky, N. E.; Manna, J. *J. Am. Chem. Soc.* **1997**, *119*, 4777. (b) Venkataraman, D.; Gardner, G. B.; Lee, S.; Moore, J. S. *J. Am. Chem. Soc.* **1995**, *117*, 11600.

(3) (a) Manna, J.; Whiteford, J. A.; Stang, P. J.; Muddiman, D. C.; Smith, R. D. *J. Am. Chem. Soc.* **1996**, *118*, 8731. (b) Slone, R. V.; Hupp, J. T.; Stern, C. L.; Albrecht-Schmitt, T. E. *Inorg. Chem.* **1996**, *35*, 4096. (c) Fujita, M.; Aoyagi, M.; Ogura, K. *Inorg. Chim. Acta* **1996**, *246*, 53. (d) Small, J. H.; McCord, D. J.; Greaves, J.; Shea, K. J. *J. Am. Chem. Soc.* **1995**, *117*, 11588.

(4) (a) Fujita, M.; Kwon, Y. J.; Washizu, S.; Ogura, K. *J. Am. Chem. Soc.* **1994**, *116*, 1151. (b) Lu, J.; Paliwala, T.; Lim, S. C.; Yu, C.; Niu, T.; Jacobson, A. J. *Inorg. Chem.* **1997**, *36*, 923. (c) Robson, R.; Abrahams, B. F.; Batten, S. R.; Gable, R. W.; Hoskins, B. F.; Liu, J. *Supramolecular Architecture*; American Chemical Society: Washington, DC, 1992; Chapter 19. (d) Subramanian, S.; Zaworotko, M. J. *Angew. Chem., Int. Ed. Engl.* **1995**, *34*, 2127. (e) Losier, P.; Zaworotko, M. J. *Angew. Chem., Int. Ed. Engl.* **1996**, *35*, 2779.

(5) 2D extended networks possessing combinations of bridging ligands have been reported. These systems do not exhibit cavities capable of entrapping guest species. (a) Decurtins, S.; Schmalte, H. W.; Schneuwly, P.; Zheng, L.-M.; Ensling, J.; Hauser, A. *Inorg. Chem.* **1995**, *34*, 5501. (b) Kawata, S.; Kitagawa, S.; Kondo, M.; Furuchi, I.; Munakata, M. *Angew. Chem., Int. Ed. Engl.* **1994**, *33*, 1759.

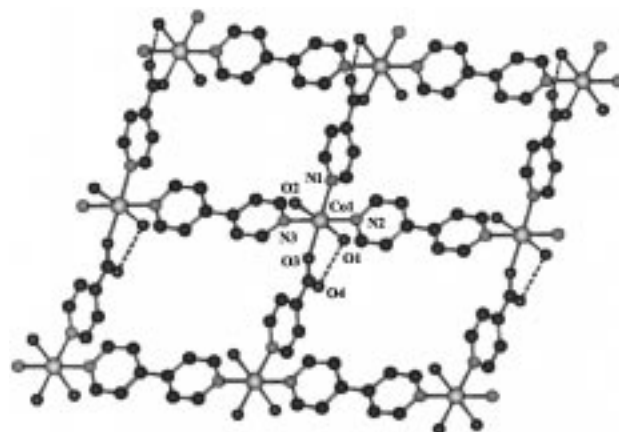
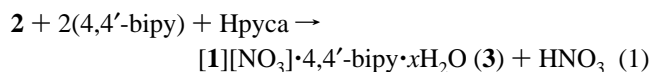


Figure 1. A view of the rectangular grids depicting the metal ion coordination in **3a**. We note that **3b** exhibits the same numbering scheme (see the Supporting Information). Selected interatomic distances (Å): Co(1)–O(1) 2.097(3), Co(1)–O(2) 2.095(3), Co(1)–O(3) 2.104(3), Co(1)–N(1) 2.166(4), Co(1)–N(2) 2.217(4), Co(1)–N(3) 2.205(4), O(4)···O(1) 2.658(5) (**3a**), Cd(1)–O(1) 2.325(4), Cd(1)–O(2) 2.317(4), Cd(1)–O(3) 2.279(4), Cd(1)–N(1) 2.327(5), Cd(1)–N(3) 2.365(5), O(4)···O(1) 2.674(6) (**3b**).

When a hot, aqueous solution (5 mL) of either $\text{Co}(\text{NO}_3)_2 \cdot 6\text{H}_2\text{O}$ (**2a**, 10.0 mg, 34.4 mmol) or $\text{Cd}(\text{NO}_3)_2 \cdot 5\text{H}_2\text{O}$ (**2b**, 9.1 mg, 34.4 mmol) was added to a hot, aqueous solution (4 mL) of 4,4'-bipy (10.7 mg, 68.8 mmol) and Hpyca (4.2 mg, 34.4 mmol) according to eq 1, crystals of **3a** (yield, 58.7%, single product) and **3b** (yield, 59.3%, single product), respectively, suitable for X-ray analysis formed upon cooling. The formulations of **3a** and **3b** were confirmed by single-crystal X-ray diffraction,⁶ thermogravimetric analysis,⁷ and analytical data.⁸



A view depicting the metal ion coordination in **3a** is shown in Figure 1. The metal center is coordinated to two trans μ -(4,4'-bipy) ligands, two trans μ -pyca ions, and two trans water molecules that form a slightly distorted octahedral coordination environment. Notably, the pyca ion participates in an O–H···O hydrogen bond with a coordinated water molecule such that its carboxylate moiety lies approximately orthogonal to the MN_3O plane.⁹ As a consequence of this arrangement, a cavity-containing rectangular grid which lies parallel to the crystallographic *ab* plane and exhibits intragrid $\text{M} \cdots \text{M}$ separations of $11.5 \times 9.2 \text{ \AA}$ for **3a**

(6) Crystal data for **3a**: crystal size $0.20 \times 0.20 \times 0.30 \text{ mm}$, monoclinic, space group $P2_1/c$, $a = 11.506(1)$, $b = 18.422(1)$, and $c = 14.598(1) \text{ \AA}$, $\beta = 97.992(1)^\circ$, $U = 3064.3(3) \text{ \AA}^3$, $2\theta_{\text{max}} = 45^\circ$, Mo $K\alpha$ radiation ($\lambda = 0.710 70 \text{ \AA}$) for $Z = 4$. Least-squares refinement based on 3642 reflections with $I_{\text{net}} > 2.0\sigma(I_{\text{net}})$ (out of 3992 unique reflections), and 402 parameters on convergence gave a final value of $R = 0.063$. Crystal data for **3b**: crystal size $0.30 \times 0.30 \times 0.40 \text{ mm}$, monoclinic $P2_1/c$, $a = 11.809(1)$, $b = 19.033(1)$, and $c = 14.344(1) \text{ \AA}$, $\beta = 98.630(1)^\circ$, $U = 3187.3(3) \text{ \AA}^3$, $2\theta_{\text{max}} = 45^\circ$, Mo $K\alpha$ radiation ($\lambda = 0.710 70 \text{ \AA}$) for $Z = 4$. Least-squares refinement based on 3335 reflections with $I_{\text{net}} > 2.0\sigma(I_{\text{net}})$ (out of 4167 unique reflections), and 400 parameters on convergence gave a final value of $R = 0.052$. Intensity data for **3a** and **3b** were collected with the use of the Siemens SMART system at 173 K.

(7) The TGA traces of **3a** and **3b** reveal gradual weight losses of 36.0% (calcd 35.5%) and 33.1% (calcd 33.5%) from 25 to 235 and 290 °C, respectively, which correspond to 3.5 (**3a**) and 4 (**3b**) molecules of H_2O and a single molecule of 4,4'-bipy, leaving behind $[\text{M}(4,4'\text{-bipy})(\text{pyca})][\text{NO}_3]$. Further decomposition leads to the corresponding oxide.

(8) Anal. Calcd for **3a** ($[\text{Co}(4,4'\text{-bipy})(\text{pyca})(\text{H}_2\text{O})_2][\text{NO}_3] \cdot 4,4'\text{-bipy} \cdot 1.5\text{H}_2\text{O}$): C, 50.49; H, 4.40; N, 13.59. Found: C, 50.25; H, 4.23; N, 14.00. Anal. Calcd for **3b** ($[\text{Cd}(4,4'\text{-bipy})(\text{pyca})(\text{H}_2\text{O})_2][\text{NO}_3] \cdot 4,4'\text{-bipy} \cdot 2\text{H}_2\text{O}$): C, 45.86; H, 4.15; N, 12.35. Found: C, 45.93; H, 4.16; N, 12.04.

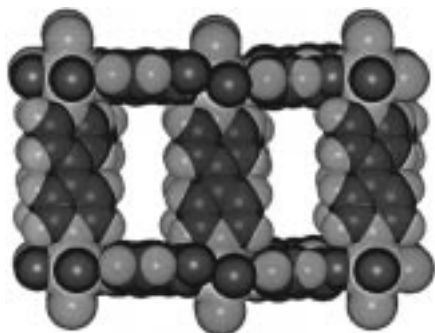


Figure 2. Space-filling view of **3a** perpendicular to the stacked layers showing the microchannels.

($11.8 \times 9.6 \text{ \AA}$, **3b**) across each 4,4'-bipy ligand and pyca ion, respectively, has formed.

A space-filling view depicting the extended structure of **3a** is shown in Figure 2. As in the square frameworks $\text{Cd}(4,4'\text{-bipy})_2(\text{NO}_3)_2 \cdot 2\text{C}_6\text{H}_4\text{Br}_2$ (**4**)^{4a} and $\text{Co}(\text{NCS})_2(4,4'\text{-bipy})_2 \cdot 2(\text{CH}_3\text{CH}_2)_2\text{O}$ (**5**),^{4b} the grids self-assemble, along the crystallographic *c* axis, to form stacked layers.¹⁰ Unlike in **5**¹¹ but as in **4**, the stacking exhibited by the grids yields microchannels that run approximately perpendicular to the layers, the dimensions of the microchannels being approximately equal to the dimensions of the rectangular cavities. In both **3a** and **3b**, the microchannels are occupied by disordered nitrate ions and disordered water molecules bound together via hydrogen-bonding interactions. Unlike in **4**, there are no appreciably strong host lattice–guest interactions between the edges of the cavities and the included guest species.^{4a,12}

Further inspection of the self-assembly exhibited by **1**, as shown in Figure 3, reveals that pyca ions of adjacent grids interact via C–H···O hydrogen bonds¹³ such that they form self-assembled dimers. As a result, the grids are aligned which, in turn, yields the microchannels that run approximately perpendicular to the layers. Interestingly, these interactions also give rise to pores (diameter $\sim 4.0 \text{ \AA}$) that interconnect the microchannels in regions

(9) The pyca ion as an *exo*-bidentate bridging ligand in the solid state: (a) Chen, Z. N.; Liu, S. X.; Qiu, J.; Wang, Z. M.; Huang, J. L.; Tang, W. X. *J. Chem. Soc., Dalton Trans.* **1994**, 2989. (b) Ng, S. W.; Das, V. G. K. *J. Crystallogr. Spectrosc. Res.* **1992**, *22*, 371. (c) Cingi, M. B.; Manfredotti, A. G.; Guastini, C.; Nardelli, M. *Gazz. Chim. Ital.* **1972**, *102*, 1034.

(10) Interpenetration by square grids has been observed in the absence of guest species. Gable, R. W.; Hoskins, B. F.; Robson, R. *J. Chem., Chem. Commun.* **1990**, 1677. See also ref 4e.

(11) The grids in **5** stack such that adjacent layers lie staggered to each other (see ref 4b).

(12) We note O–H···O hydrogen bonds between coordinated water molecules and nearest-neighbor guest water molecules. The remaining guests, however, are highly disordered despite data collection at 173 K.

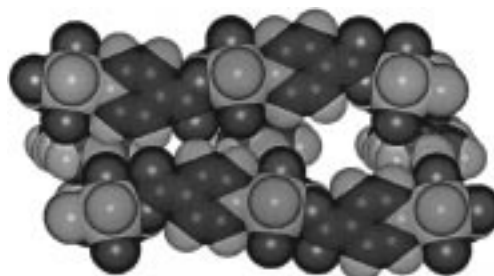


Figure 3. Space-filling view of **3a** parallel to the stacked layers depicting the self-assembly displayed by the pyca ions. The left side of the figure shows the self-assembled dimers while the right side shows the pores that connect the microchannels.

where pyca ions of adjacent layers do not assemble to form dimers. Owing to the ability of these interactions to push the layers apart, free molecules of 4,4'-bipy have also assembled between the grids and engage in O–H···N hydrogen bonds and π – π interactions with coordinated water molecules and coordinated 4,4'-bipy ligands of adjacent layers, respectively.¹⁴ Thus, **3** possesses interconnected microchannels in a similar way to that exhibited by host zeolite lattices.¹⁵

The results reported herein illustrate a new extension to the chemistry of cavity-containing square assemblies. By selecting two unique bridging ligands, we have shown that the design of cavity-containing rectangular grids (**1**), which lead to interconnected microchannels, may be achieved using the principles of self-assembly. We anticipate this approach to be viable for the construction of cavity-containing rectangular frameworks possessing bridging ligands not described here, and we also anticipate this approach to be applicable for the design of *discrete* rectangular assemblies.³ Current efforts are underway to explore further inclusion properties of **1**.

Acknowledgment. We are grateful for funding from the National Science Foundation and the Natural Sciences and Engineering Research Council of Canada (NSERC) for a doctoral fellowship (L.R.M.).

Supporting Information Available: Crystallographic reports and tables of positional and thermal parameters, and bond lengths and angles, and TGA traces for **3a** and **3b** (16 pages, print/PDF). See any current masthead page for ordering information and Web access instructions.

JA973584M

(13) Desiraju, G. R. *Acc. Chem. Res.* **1996**, *9*, 441.

(14) The inclusion of 4,4'-bipy within **3** also produces walls that span the lengths of the microchannels.

(15) Meier, W. M.; Olson, D. H. *Atlas of Zeolite Structure Types*, 3rd ed.; Butterworth-Heinemann: Boston, MA, 1992.